

MAGNETIC TESTING STAND CONSTRUCTION AND INITIAL TESTING

BY

JOHAN POTGIETER¹, EDDIE RODGERS¹ and IOAN TULEAȘCĂ^{*,2}

¹School of Engineering and Advanced Technology, Massey University,
Auckland, New Zealand

²Engineering & Construction Centre, Open Polytechnic of New Zealand

Received, January 10, 2012

Accepted for publication: March 6, 2012

Abstract. A method of associating the Fibonacci sequence and the golden ratio with designing a magnetic testing stand was developed. Applying this concept a magnetic testing stand was built using custom made magnets and original manufacturing concepts. The materials used for building the base structure of the prototype were non magnetic (Perspex, High Density Polyethylene – HDPE, Medium Density Fibreboard – MDF). The proposed dimensions were loosely followed, since cost-related, technological, mechanical and strength constraints had to be observed.

Key words: magnetic testing stand; technology; non-magnetic materials; built-in testing variables; test results.

1. Introduction

Using the results obtained in a previous work (Tuleașcă *et al.*, 2011) as a starting point, a magnetic testing stand was built and preliminary tests were performed. The magnetic testing stand comprises four main parts: *the base structure, the static structure, the rotating (mobile) structure and the driving and control part.*

*Corresponding author: *e-mail*: ioan.tuleasca.openpolytechnic.ac.nz@yahoo.com

The *mobile structure* is made up in three layers of rotating cylinders embedded in frames driven by electrical motors and the *static structure* comprises three concentric rings. The cylinders and the rings have similar make up: two concentric layers of neodymium N45 (that have specific, longitudinal and radial, magnetization patterns), a layer of High Density Polyethylene (HDPE) and a layer of aluminium.

The magnetic parts of the cylinders and rings were supplied by Magnets New Zealand Ltd, who also assembled the magnetic components of the cylinders.

The magnetic components of the rings were assembled at Massey University Albany Workshop. The process was sophisticated and involved some manufacturing novelties as to avoid damage to the magnetic parts and also to ensure mechanical stability.

The magnetic parts of the cylinders and rings were embedded in HDPE and aluminium layers resulting in the *static* and *mobile structures* and a *base structure* was built around these components (also at Massey University Albany Workshop).

Achieving the best driving capability for the *driving and control part* assigned to the stand involved testing DC and AC motors to ascertain the most suitable option for reaching adequate torques and angular velocities. Eventually, three AC motors and associated controllers were chosen that enabled the three frames to reach not only mechanical stability but also increased angular velocities.

2. Description of the Stand

2.1. Base Structure

The *base structure* was built with non-magnetic materials, mainly wood and MDF, to avoid magnetic interferences. It also includes four bottle jacks used to lower and secure the *static structure* containing the rings into position.



Fig. 1 – The base structure.

It was decided to attach the *rotating (mobile) structure* to the *base structure* via shafts that transmit the motion from electrical motors. Complementing this decision was the option taken for the *static structure* containing the rings to be lowered from above the stand into the frames containing cylinders of the *mobile structure*, enhancing stability and controllability of the whole experimental process. These were fundamental technical decisions that provided a sound starting point for the subsequent phases of the technological and manufacturing processes.

2.2. Static Structure

The *static structure* is made in three concentric magnetic rings (shown in Fig. 2, where a special magnetic paper is used to emphasize the magnetic fields appearance). The rings are attached to a Perspex structure that allows visibility as well as enough strength to keep the rings into the upside down position required by the building constraints. They are made of (from center to exterior) two concentric layers of neodymium N45 (that have specific, longitudinal and radial, magnetization patterns), a layer of HDPE and a layer of aluminium.

The alternating N-S radial positioned poles (around the N-S oriented longitudinal magnets) magnetizing option was chosen (Tuleașcă *et al.*, 2011), where the radial magnets have 16 alternating, radial oriented, N-S poles, components (Appendix 1).

The rings were assembled at the Massey University Workshop using custom made jigs and dedicated technology. No damage to the magnetic parts was produced, which demonstrates the accuracy of the process.

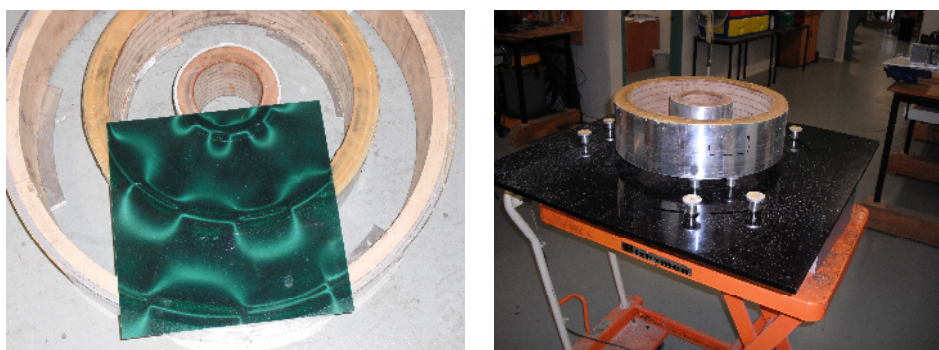


Fig. 2 – The rings and the Perspex plate.

a) *Static Structure Magnetic Component Manufacturing Process*

The neodymium N45 magnets of the rings are bonded into position using tooling jigs (supporting structures) that are made in MDF (Medium Density Fibreboard) and the manufacturing process has two components:

Process A – the one associated with the longitudinal magnetic field parts.

Process B – the one associated with the radial magnetic field parts.

Each jig is made up in six radial superposed layers (with $D_{\text{ext}} \gg D_{\text{int}}$). Each layer contains half pieces glued together. The seams of each layer fall in the middle of adjacent layers for strengthening purposes. The six layers are glued to a polyester resin base for increased stability ($D_{\text{PR}} \gg D_{\text{ext}}$). The base is used only for manufacturing purposes and is subsequently removed. The described supporting structure is built and then machined to desired dimensions, specific for each ring. The final magnetic arrangement is reflected in Fig. 3.

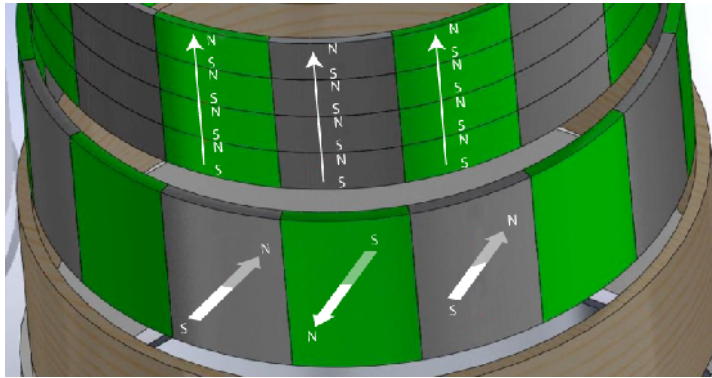


Fig. 3 – Exploded view of magnets arrangement.

Details of Process A. Semi circle MDF rings are glued together to form the supporting wood ring seen in Fig. 4. Grooves are subsequently cut to allow every second stack of four magnets to be inserted around the outside of the ring (Fig. 5). With all the magnets placed in grooves, the wood between the magnets is removed to make room for the next lot of magnets (Fig. 6).

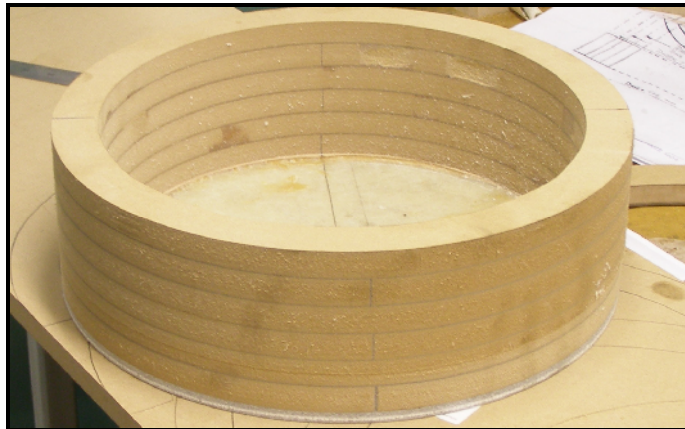


Fig. 4 – Inner wooden ring.



Fig. 5 – Grooves for magnets.

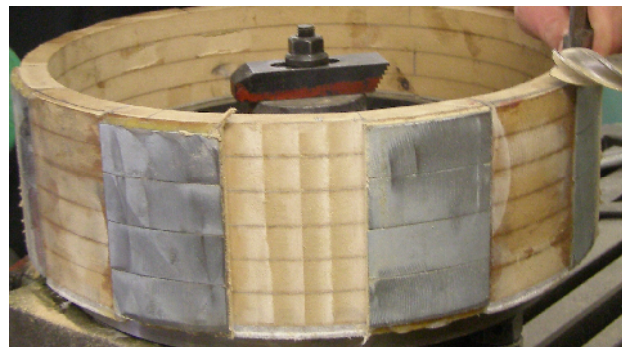


Fig. 6 – First set of magnets in place.

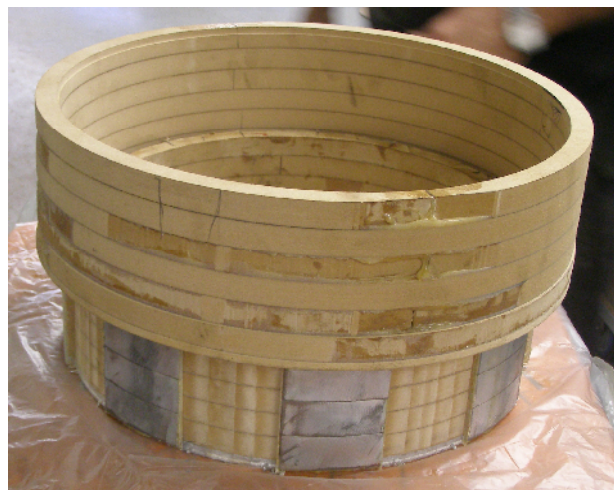


Fig. 7 – Placing outer wood ring over assembly.

After every second magnet of the first layer is glued to the wood frame a second larger wooden frame is placed around the assembly, encasing the magnets (Fig. 7). This means that the next lot of magnets can be positioned

without interference from the magnetic fields of the first set already on the ring. The remaining magnets are then inserted with liberal amounts of glue as it is of great importance that they do not move once in position (Fig. 8).

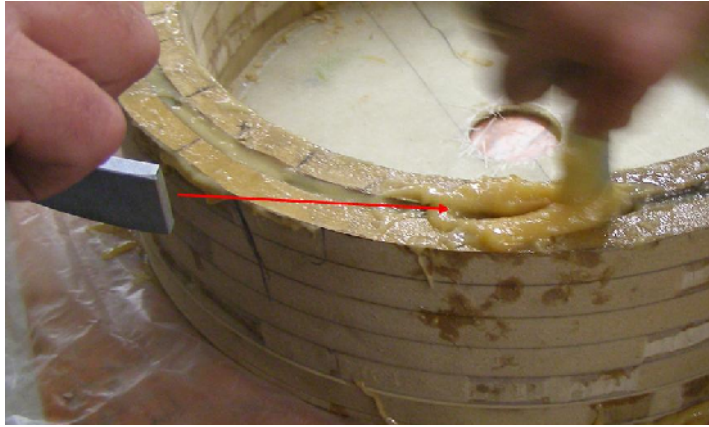


Fig. 8 – Inserting magnets to finish the first layer.

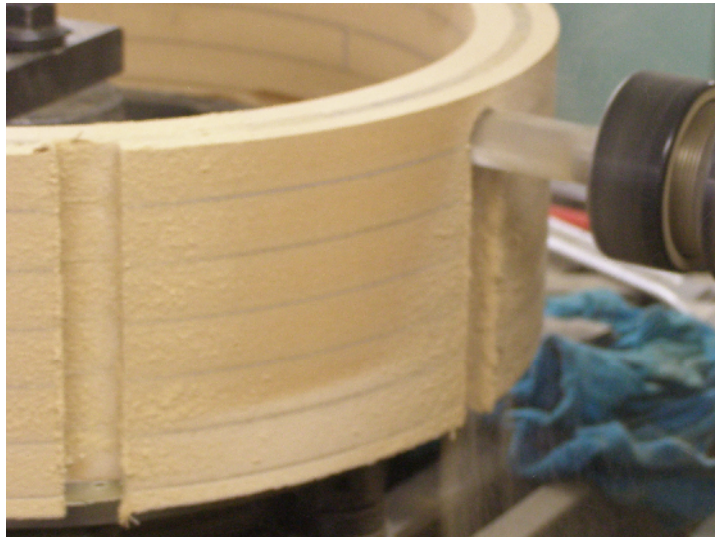


Fig. 9 – Starting grooves for the second layer of magnets.

Details of Process B. Once *Process A* is complete the operation (Fig. 9) is repeated for *Process B* magnets, which comprises 16 radial magnetized components. Effectively the ring of wood between *Process A* magnets and *Process B* magnets is completely removed and is not part of the finished prototype. It is used only as a way of securing the structure until the magnets are fixed in position. However, the *Process B* radial magnets do not possess an

outer MDF ring and the magnets filling the gaps are held in place by clamps, as seen in Fig. 10. Also, a thin layer of wood is added to the inside, top, and outside, of the ring, as seen in Fig. 11.



Fig. 10 – Clamping the radial magnets in place.



Fig. 11 – Clamping a thin wooden inner layer in place.

Once the magnets are encased in the MDF tooling jig the assembly of the remaining HDPE and aluminium layers becomes much less difficult.

Fig. 12 shows the renderings of a complete ring both in exploded and assembled views. The rings are attached to a Perspex plate (base) with even

spacing between them. They are mounted on slotted holes so that for fine tuning they can be rotated with 22° in order to appropriately align the magnetic fields and to maximize the performance of the unit.

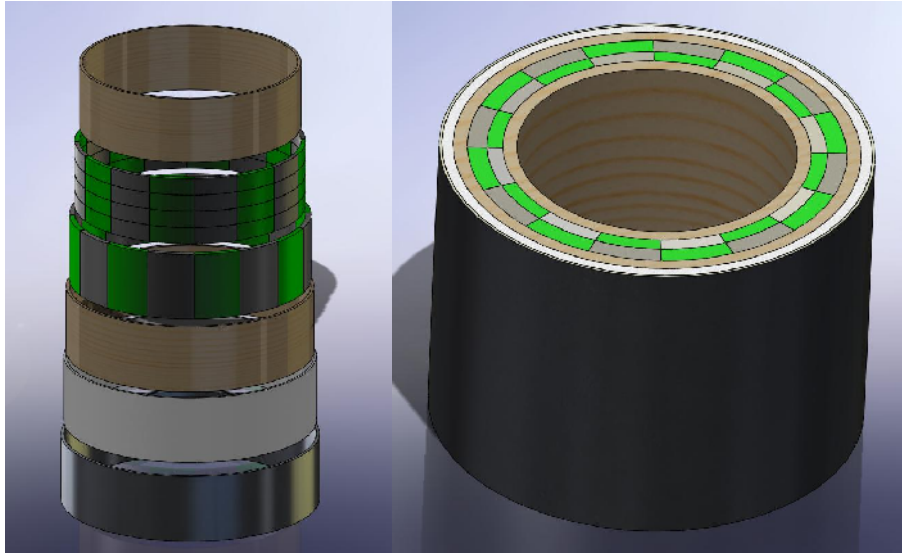


Fig. 12 – Renderings of a fully assembled ring.

2.3. Rotating (Mobile) Structure

The rotating structure comprises three concentric frames made in Perspex (Fig. 13) that rotate around the rings and support purpose made magnetic cylinders (Fig. 14). Driven by the frames, the cylinders spin both around the rings and around their axes.



Fig. 13 – Concentric frames containing the cylinders.

The cylinders are made of (from center to exterior) two concentric layers of neodymium N45 (that have specific, longitudinal and radial,

magnetization patterns), a layer of HDPE and a layer of aluminium.

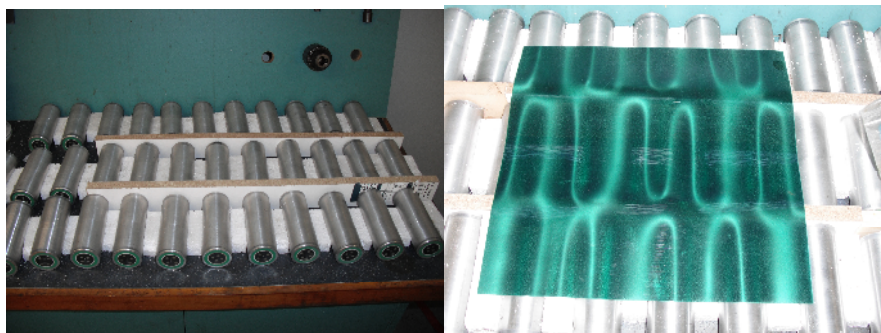


Fig. 14 – Cylinders and their magnetic field configuration.

The alternating N-S radial positioned poles (around the N-S oriented longitudinal magnets) magnetizing option was chosen as well (Tuleașcă *et al.*, 2011), where the cylinders' radial magnets have four alternating, radial oriented, N-S poles, components (Appendix 1).

2.4. The Driving and Control Part

The *driving and control part* consists of three AC motors (two 3-phase 0.55 kW MOT BN71C4, one 3-phase 1.5 kW TECO D90 Alloy Frame) and associated gear boxes (Fig. 15), driven by suitably matched controllers (two



Fig. 15 – The three AC motors that rotate the frames.

Bonfiglioli Vectron SYN 10 S220 05 AF IP65S, one Bonfiglioli Vectron SYN 10 S220 07 AF IP65F), (Fig. 16). Gear boxes are attached to the motors to provide for appropriate torque and speed. The motion is transmitted to the frames' driving shaft *via* belts and sprockets.

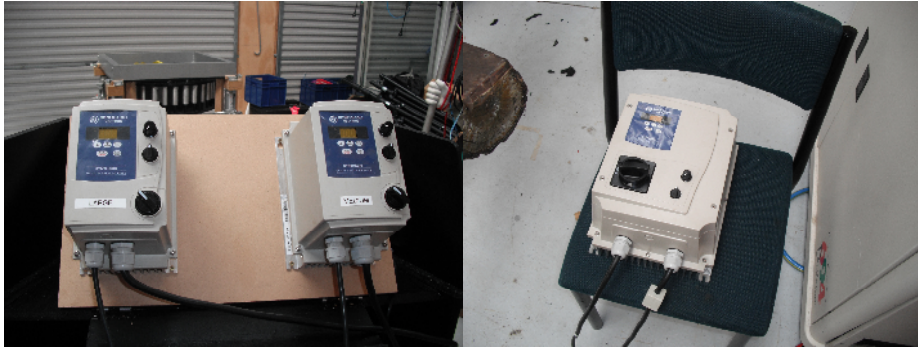


Fig. 16 – The Bonfiglioli Vectron controllers associated with the AC motors.

It has to be mentioned that the electrical motors selection process started with PWM (MOSFET based) speed controlled 40 V DC motors (which proved ineffective), followed by readily available low rated AC motors and associated controllers (XTRAVERT 702, 704 and TVERTER E2) and ending with the three motor-controller units described above (last one bought in September 2010).

2.5. Built in Testing Variables

A number of variables that need to be modified and correlated during tests were embedded into the stand construction, through adequate design and execution:

- a) the rings' position, that can be circularly modified on an angle of 22° on the Perspex plate;
- b) the number of cylinders that can be associated with each frame (two sequences were proposed 13-21-34 cylinders and 8-13-21 cylinders, where adequately spaced slots were machined in the frames to accommodate the cylinders);
- c) the relative position of the longitudinal magnetic field N-S of the cylinders and rings, that can match or can be in opposition;
- d) the speed with which the three frames rotates around the rings;
- e) the direction that the three rotating frames can have (clockwise or/and anticlockwise);
- f) the relative position of the array of cylinders, where the cylinders can be mounted around three different diameters on the associated frame;
- g) the depth at which the rings assembly is inserted into the frames assembly containing the cylinders.

The variables enhance the experimental capabilities of the stand and its testing versatility.

3. Testing and Further Developments

Tests were performed to determine, in the first place, mechanical and electrical limitations, and then to ascertain whether, in the present make up, the magnetic testing stand can achieve the sought after specific physical effects. The tests implied rotating the frames around the fixed rings at varying velocities, in such a manner that no thermal or mechanical damage was sustained by the system.

As already mentioned, tests started with 40 V DC electrical motors driven by PWM, MOSFET based, controllers. Especially due to low torques developed by these motors but also to electric and magnetic field interferences, the electronic circuitry did not withstand the high value of electrical currents required and was damaged during tests.

Subsequently, low rated AC motors (under 0.5 kW) attached to custom made gear boxes and associated controllers (XTRAVERT 702, 704 and TVERTER E2) were tested, however the torque provided by these motors was also insufficient.

Finally, the decision was taken to purchase new AC motors (two 3-phase 0.55 kW MOT BN71C4, one 3-phase 1.5 kW TECO D90 Alloy Frame) and associated controllers (two Bonfiglioli Vectron SYN 10 S220 05 AF IP65S, one Bonfiglioli Vectron SYN 10 S220 07 AF IP65F), that were tested and their maximum velocities were ascertained (Appendix 2).

As it can be seen, mechanical stability was achieved for all three units, however the speed could not exceed 160 rpm for the large and the medium units.

Temperature testing was also performed (by an AINDT qualified specialist thermographer) using a thermal camera, with un-conclusive results (small variations, between 0.1 to 0.6°C, were registered, which could have been engendered by environment perturbations).

Magnetic fields visualization was performed using Magnaview special paper however the rendition was acceptable only for static magnetic fields and slightly visible for the locus of the rotating magnetic fields. No spatial evolution of the magnetic fields around the stand was able to be visualized since no technical equipment can perform this task yet.

Soft iron sheets ($5 \times 1.2 \text{ mm} = 6 \text{ mm}$ width) will be attached to the three rings and to the cylinders with the aim of enhancing the magnetic fields. Tests will subsequently be performed, where purchasing and attaching 1.5 kW motors and associated controllers to replace the 0.55 kW ones, as well as using more robust Polycarbonate plates instead of the Perspex ones, are options for safely increasing the angular velocity.

4. Conclusions

A magnetic testing stand was built following the paradigm developed by Tuleaşcă *et al.* (2011) and initial tests were performed. Due to cost-related, technological, mechanical and strength constraints that had to be observed the dimensioning and materials choosing processes were influenced. Consequently, the initial stages of the research, as presented in the paper, focused mostly on effectively associating the theoretical concepts with the practicality of building a novel experimental device, and on devising original technical solutions to:

a) safely and effectively assemble the magnetic components of the stand;

b) organize the construction and interaction of the *mobile* and *static structures* of the stand, where the *static structure* containing the rings comes from above and slides into the *mobile structure* containing the cylinders;

c) provide, *via* adequate design and execution, of embedded variables in the structure of the stand (slots in the Perspex material to enable the rings to be circularly shifted on an angle of 22° , holes in the Perspex frame for the cylinders to be shifted in three different radial positions around the circumference as well as for two different sequences, 13-21-34 cylinders and 8-13-21 cylinders, the possibility to reverse the magnetic field direction of the cylinders by easily changing their polarity);

d) use cost effective and weight saving solutions to hold the cylinders into position and enable them to rotate safely at extremely high angular velocities (two pins that rotate freely on Vesconite, one on top and the other on the bottom of the cylinder, make the connection with the Perspex frame);

e) offer adequate speed control and torque stability to the driving process by attaching gears (including custom made gears) to the AC motors.

The tests already performed proved the validity of the engineering solutions and of the technological processes developed for building the magnetic testing stand. It can be ascertained that the stand is capable of withstanding increased mechanical constraints that further experiments may need to achieve.

Appendix 1

Magnets details

1. Neodymium cylinders dimensions

The neodymium cylinders are made up of two pieces:

a) the interior one, in the shape of a cylinder ($D_{\text{int}} = 10$ mm, $H = 110$ mm), is magnetized with a longitudinal N-S magnetic field (Fig. A1);

b) the exterior one, in the shape of a ring ($D_{\text{int}} = 10$ mm, $D_{\text{ext}} = 26$ mm, $H = 110$ mm), is magnetized with a radial magnetic field, and has four alternating N-S poles (Fig. A2).

The two parts are bonded together forming the neodymium layer.

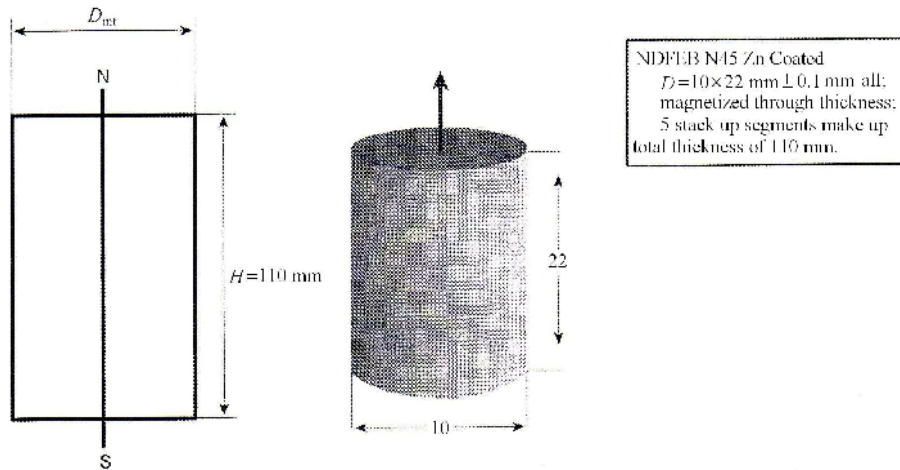


Fig. A1 – Longitudinal magnetic field.

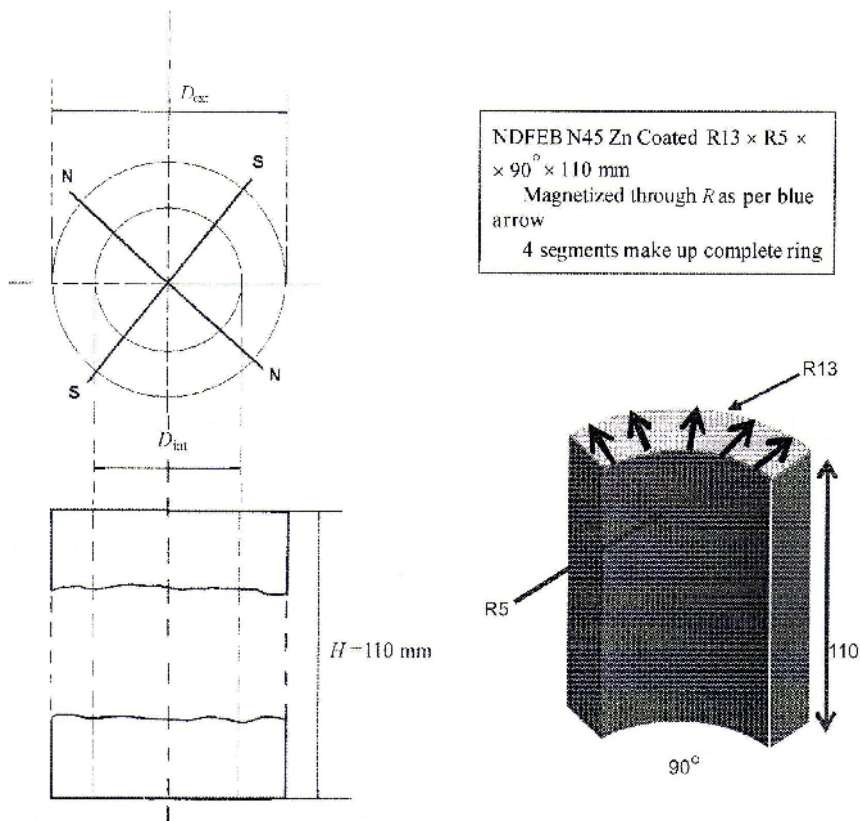


Fig. A2 – Radial magnetic field (4 poles).

2. Neodymium rings dimensions

The neodymium rings are made up of two parts:

a) the interior one, comprising 4 stacks of 16 pieces each, displays a longitudinal N-S magnetic field (Fig. A3);

b) the exterior one, comprises 16 radial magnetized pieces, alternately N-S positioned on the circumference (Fig. A4).

The two parts are bonded together forming the neodymium layer.

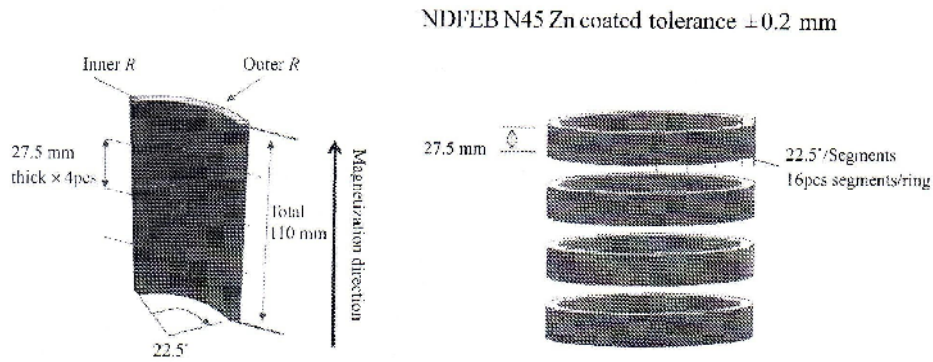


Fig. A3 – Longitudinal magnetic field.

Table A1

	Outer R mm	Inner R mm	Thickness mm	No. of pieces to build a complete ring (Rows \times Segments 22.5°)
Size R 1-1	60	55	27.5	4 \times 16 = 64 pcs
Size R 2-1	183	178	27.5	4 \times 16 = 64 pc
Size R 3-1	306	301	27.5	4 \times 16 = 64 pc

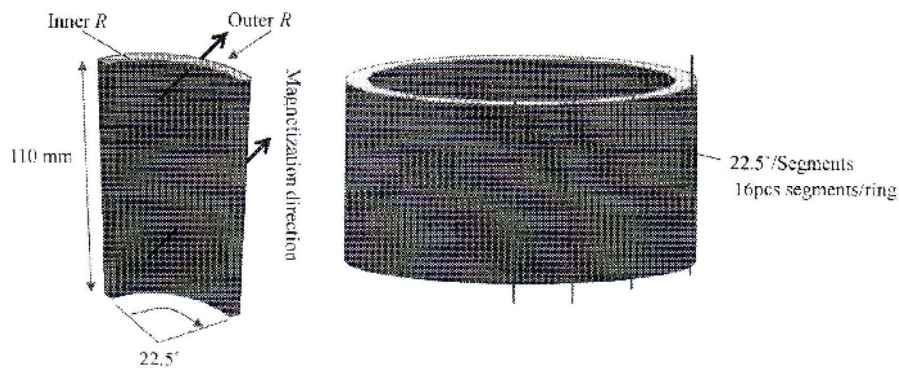


Fig. A4 – Radial magnetic field (16 poles).

Table A2

	Outer R mm	Inner R mm	Thickness mm	No. of pieces to build a complete ring (Rows \times Segments 22.5°)
Size R 1-2	68	60	110	$1 \times 16 = 64$ pcs
Size R 2-1	191	183	110	$1 \times 16 = 64$ pcs
Size R 3-1	314	306	110	$1 \times 16 = 64$ pcs

Appendix 2**Experimental Results***1. Large Frame*

Motor: 3-phase 0.55 kW MOT BN71C4.

Controller: Bonifiglioli Vectron SYN 10 S220 05 AF IP65S.

Table A3

Controller frequency, [Hz]	Frame speed, [rpm]	Observations
100	75	
105	78.7	
110	82.6	
115	85.8	
120	88.7	
125	92.9	
130	96	
135	98.6	
140	101.2	Stability achieved
145	104.3	
150	106.5	
155	107.5	
160	Limit achieved	Default stop

2. Medium Frame

Motor: 3-phase 0.55 kW MOT BN71C4.

Controller: Bonifiglioli Vectron SYN 10 S220 05 AF IP65S.

Table A4

Controller frequency, [Hz]	Frame speed, [rpm]	Observations
100	103	
120	121	
125	125.5	
130	129.5	
135	133.9	
140	138	Stability achieved
145	141	
150	Limit achieved	Default stop

3. Small Frame

Motor: 3-phase 1.5 kW TECO D90 Alloy Frame.

Controller: Bonifiglioli Vectron SYN 10 S220 05 AF IP65F.

Table A5

Controller frequency, [Hz]	Frame speed, [rpm]	Observations
50	107	
70	150	
90	192	Stability achieved
100	215	
120	257	
140	297	
145	307	
150	316.5	
155	329	
160	338.5	
165	345.5	
170	357	
175	365 – tests stoped	Safety limit supposedly reached

REFERENCES

- Burnett D., *143.485 Engineering Project*. Project Report, Massey Univ., Albany Campus, New Zealand, January 2010.
- Moskowitz L.R., *Permanent Magnet Design and Application Handbook*. Krieger Publ. Comp., Malabar, FL, USA, 1995.
- Tuleaşcă I., Potgieter J., Burnett D., *Magnetic Testing Stand Design Using the Fibonacci Sequence and the Golden Ratio*. Bul. Inst. Politehnic, Iaşi, **LVII (LXI)**, 4, s. Electrot., Energ., Electron. (2011).
- Tuleaşcă I., Potgieter J., *Does Maxwell's Complete System of Equations Reflect the Interconnection between Electric, Magnetic and Gravitational Fields?* Marsden Fund Prelimin. Res. Proposal, February 2011.
- * * * *TVERTER E2 Adjustable Speed Driver Operations Manual*. TECO Electric & Machinery Co. Ltd., 4KA72X025T01 Ver: 09 2005.08.
- * * * *XTRAVERT Series Technical Manual*. MGI Technologies Inc., PDL Electronics Ltd., 4201-196 Rev F.
- * * * *Synthesis Operations Manual*. Bonfiglioli Vectron, COD. VEC 114 R1.

CONSTRUCȚIA UNUI STAND DE TESTĂRI MAGNETICE ȘI TESTE INIȚIALE

(Rezumat)

Bazat pe un proiect anterior ce folosea numărul de aur și seria lui Fibonacci pentru dimensionarea unui dispozitiv de cercetări magnetice, a fost construit un stand de testări. Standul este realizat prin folosirea unei tehnologii originale și are patru părți principale: structura de rezistență, partea fixă, partea mobilă și grupul de control și acționare. Partea fixă și cea mobilă conțin materialele de lucru (compozite) ce produc câmpuri magnetice specifice, a căror interacțiune se urmărește. Sunt prezentate rezultate ale testărilor inițiale și sunt indicate următoarele etape ale cercetării.